

Article

Synthesis and Evaluation of the Antifungal and Toxicological Activity of Nitrofurans Derivatives

Carolina Orlando Vaso ^{1,†}, Fabiana Pandolfi ^{2,†}, Niura Madalena Bila ¹, Daniela De Vita ³, Martina Bortolami ², Maria José Soares Mendes-Giannini ¹, Valeria Tudino ⁴, Roberta Costi ⁵, Caroline Barcelos Costa-Orlandi ¹, Ana Marisa Fusco-Almeida ^{1,*} and Luigi Scipione ^{4,*}

¹ School of Pharmaceutical Science, Universidade Estadual Paulista, Araraquara 14800-903, SP, Brazil; carolvaso@hotmail.com (C.O.V.); niura.madalena.bila@gmail.com (N.M.B.); maria.giannini@unesp.br (M.J.S.M.-G.); carolbarceloscosta@gmail.com (C.B.C.-O.)

² Department of Scienze di Base e Applicate per l'Ingegneria, Sapienza University of Rome, Via Castro Laurenziano 7, 00185 Rome, Italy; fabiana.pandolfi@uniroma1.it (F.P.); martina.bortolami@uniroma1.it (M.B.)

³ Department of Environmental Biology, Sapienza University of Rome, Piazzale Aldo Moro 5, 00185 Rome, Italy; daniela.devita@uniroma1.it

⁴ Department of Chimica e Tecnologia del Farmaco, Sapienza University of Rome, Piazzale Aldo Moro 5, 00185 Rome, Italy; valeria.tudino@uniroma1.it

⁵ Department of Chemistry and Technology of Drug, Istituto Pasteur, Fondazione Cenci Bolognetti, Sapienza University of Rome, Piazzale Aldo Moro 5, 00185 Rome, Italy; roberta.costi@uniroma1.it

* Correspondence: ana.marisa@unesp.br (A.M.F.-A.); luigi.scipione@uniroma1.it (L.S.)

† These authors contributed equally to this work.



Citation: Vaso, C.O.; Pandolfi, F.; Bila, N.M.; De Vita, D.; Bortolami, M.; Mendes-Giannini, M.J.S.; Tudino, V.; Costi, R.; Costa-Orlandi, C.B.; Fusco-Almeida, A.M.; et al. Synthesis and Evaluation of the Antifungal and Toxicological Activity of Nitrofurans Derivatives. *Pharmaceutics* **2022**, *14*, 593. <https://doi.org/10.3390/pharmaceutics14030593>

Academic Editor: Juan José Torrado

Received: 8 February 2022

Accepted: 4 March 2022

Published: 8 March 2022

Publisher's Note: MDPI stays neutral with regard to jurisdictional claims in published maps and institutional affiliations.



Copyright: © 2022 by the authors. Licensee MDPI, Basel, Switzerland. This article is an open access article distributed under the terms and conditions of the Creative Commons Attribution (CC BY) license (<https://creativecommons.org/licenses/by/4.0/>).

Abstract: Fungal diseases affect more than 1 billion people worldwide. The constant global changes, the advent of new pandemics, and chronic diseases favor the diffusion of fungal pathogens such as *Candida*, *Cryptococcus*, *Aspergillus*, *Trichophyton*, *Histoplasma capsulatum*, and *Paracoccidioides brasiliensis*. In this work, a series of nitrofurans derivatives were synthesized and tested against different fungal species; most of them showed inhibitory activity, fungicide, and fungistatic profile. The minimal inhibitory concentration (MIC₉₀) values for the most potent compounds range from 0.48 µg/mL against *H. capsulatum* (compound 11) and *P. brasiliensis* (compounds 3 and 9) to 0.98 µg/mL against *Trichophyton rubrum* and *T. mentagrophytes* (compounds 8, 9, 12, 13 and 8, 12, 13, respectively), and 3.9 µg/mL against *Candida* and *Cryptococcus neoformans* strains (compounds 1 and 5, respectively). In addition, all compounds showed low toxicity when tested in vitro on lung cell lines (A549 and MRC-5) and in vivo in *Caenorhabditis elegans* larvae. Many of them showed high selectivity index values. Thus, these studied nitrofurans derivatives proved to be potent against different fungal species, characterized by low toxicity and high selectivity; for these reasons, they may become promising compounds for the treatment of mycoses.

Keywords: broad-spectrum antifungal; nitrofurans derivatives; antifungal activity; *Candida* sp.; *Cryptococcus neoformans*; *Histoplasma capsulatum*; *Paracoccidioides brasiliensis*; *Trichophyton rubrum*; *Trichophyton mentagrophytes*; *Caenorhabditis elegans* larvae

1. Introduction

Fungal diseases annually affect more than 1 billion people worldwide. These infections present a wide variety of symptoms, but they can often become invasive, especially in immunocompromised patients, with the risk of leading to death. Their mortality rate is highly relevant, as it represents more than 1.6 million deaths annually, similar to the tuberculosis mortality rate and three times higher than that recorded for malaria. Fungal diseases have increased due to the number of susceptible individuals, including people living with the human immunodeficiency virus (HIV), hematopoietic stem cell or organ transplant recipients, patients with malignancies, or immunological conditions receiving immunosuppressive treatment, premature neonates, and the elderly. More recently, the

SARS-CoV-2 (COVID-19) virus pandemic has been associated with some cases of fungal diseases in hospitalized patients [1–5].

Fungal pathogens such as *Candida* and *Cryptococcus* are distributed worldwide and constitute the majority of invasive fungal infections (IFIs). Dimorphic fungi, such as *Histoplasma capsulatum* and *Paracoccidioides* spp., are geographically restricted to their respective habitats and cause endemic mycoses. Dermatophytosis is globally considered the most common dermatological disease [6].

Among these fungal diseases, candidiasis, caused by yeasts of the *Candida* genus, commonly affects the gastrointestinal tract, urinary tract, and oral cavity or becomes systemic, affecting the entire organism [7]. The annual incidence of candidiasis is around 2 million cases, and the disseminated figure is around 700,000 cases [1]. *Candida albicans* is the most prevalent species; however, lately, non-*albicans* species have increased significantly. The ascendant species are *C. parapsilosis*, *C. tropicalis*, *C. krusei*, *C. glabrata*, *C. guilliermondii* [6–9], as well as *C. auris*. *Candida* species infections are usually treated with drugs from the class of polyenes (amphotericin B and nystatin), and azoles, such as fluconazole, clotrimazole, and miconazole [7]. However, reports of fungal resistance have already been described for the standard antifungal classes used in therapy. Regarding polyenes, mutations change the principal sterol in the membrane, affecting the polyene binding, whereas, for the azole class, mutations in the gene encoding the target protein, or its overexpression, as well as other resistance mechanisms can occur [10–12]. In addition, reports of high toxicity and drug interactions are prevalent and have been described for these antifungal classes [13–15].

Encapsulated yeasts represent 200,000 cases of fungal diseases annually, mainly in individuals with the human immunodeficiency virus (HIV) [16]. The main species is *Cryptococcus neoformans* [17,18], capable of causing severe meningoencephalitis [19,20]. The most common treatment available is based on the application of polyenes, azoles, and flucytosine, depending on the severity and immunological status of the host [21,22]. When the fungus reaches the central nervous system, the main challenge in the treatment is for the drug to cross the blood-brain barrier. Amphotericin B is the most commonly indicated treatment; however, it requires hospitalization and the monitoring of liver and kidney function [21]. Cases of antifungal resistance have been reported for *Cryptococcus* sp. and reports of host toxicity, which are aggravated by a long period of treatment [21,23,24].

Histoplasma capsulatum and *Paracoccidioides* sp. cause respiratory illnesses that can become widespread [25,26]. The annual incidence of histoplasmosis is around 500,000 cases. It is a mycosis considered to have a worldwide distribution, already having been described in all continents except for Antarctica [1,27]. Paracoccidioidomycosis is an endemic infection in Latin America, and most cases occur in Brazil, Argentina, Colombia, Ecuador, Venezuela, and Paraguay [28,29]. The standard treatment for both mycoses is amphotericin B and itraconazole; however, the antibacterial cotrimoxazole (sulfamethoxazole/trimethoprim combination) is also indicated for paracoccidioidomycosis [30–33]. Cases related to nephrotoxicity, hepatotoxicity, and drug interactions increase considerably in these diseases, as they are considered systemic and require long treatments that can last for up to 24 months [26,31,33,34].

Dermatophytosis is caused by filamentous fungi that have a predilection for keratin. They mainly affect fur, hair, nails, and skin [35,36]. These mycoses affect about 20 to 25% of the world's human population [8,37]. *Trichophyton rubrum* and *T. mentagrophytes* are the most prevalent [37,38]. The usual treatment is carried out with drugs from the family of azoles and allylamines. However, prolonged treatment time, recurrent infections, and frequent reports of resistant strains to conventional drugs are the main limitations in the treatment of these mycoses [38–40].

The search for new molecules capable of effectively treating fungal infections and causing minimal toxicity is constant. Among these molecules, nitrofurans are compounds with a 5-nitrofur ring and different substituents in position 2. The first nitrofuran was described in 1944, and these drugs were widely used for decades in the field of agriculture to prevent and control diseases and were added to animal feed to stimulate growth [41,42].

In the 1990s, Europe banned the use of nitrofurans for agricultural purposes, and later in 2002, other countries such as the United States and China also banned them for animal use, due to the residues that these drugs left behind in the meat. These residues possibly cause side effects in human beings, such as hematological abnormalities (aplastic anemia), in addition to their carcinogenic, mutagenic, and genotoxic effects. Currently, many research groups have been studying nitrofuran formulations, trying to reduce their toxicity and side effects, as they have excellent antimicrobial activity [41,43,44].

There are few reports in the literature on the study of the antifungal activity of nitrofurans; some authors have shown a potent antifungal and anti-biofilm activity against *Candida* species, with the capacity to inhibit cell adhesion and aggregation [45,46]. Regarding the toxicity assessment, some studies with nitrofuran derivatives have shown that these compounds have low toxicity when tested on human cell lines [45–47].

In this study, we synthesized a series of ester, amide, or chalcone 5-nitrofuran derivatives, as depicted in Figure 1, intending to assess their antifungal activity against a wide range of fungal species and to evaluate their toxic effects on human cells in vitro and on *Caenorhabditis elegans* larvae in vivo.

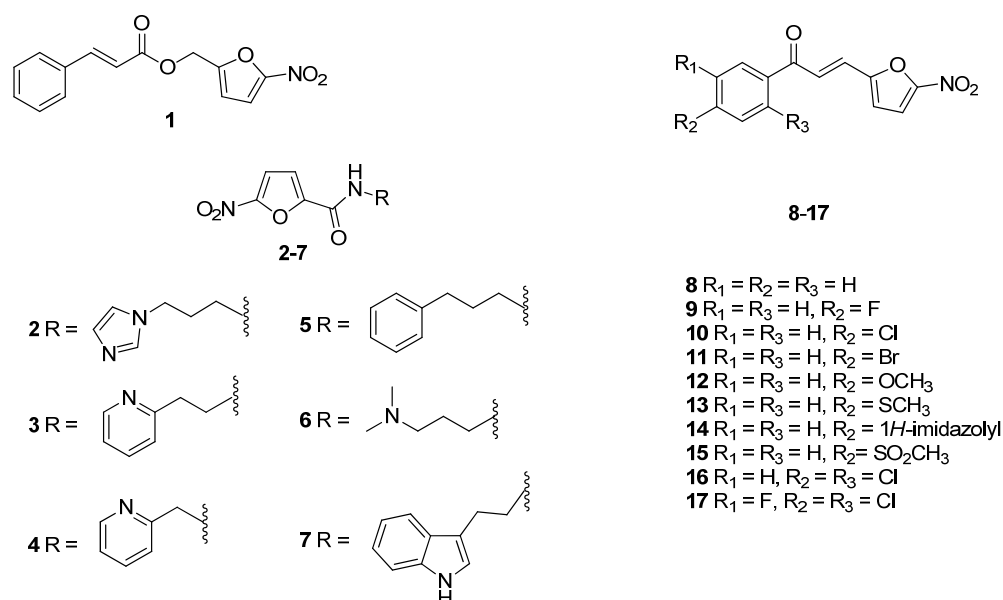


Figure 1. The nitrofuran derivatives, 1–17, as studied in this work.

2. Materials and Methods

2.1. Chemical Synthesis

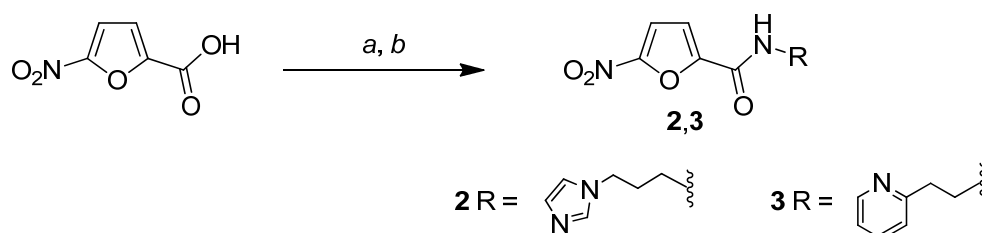
The compounds **1**, **4–14** were synthesized according to the literature (**1** [45], **4** [48], **5** [49], **6** [50], **7** [51], **8–12** [52], **13–14** [53]), and all the analytical data were in accordance with those reported previously (Table S1). The compounds **2**, **3** [54], and **15–17** [55,56] were not previously described and were synthesized following literature methods; the detailed chemical procedures and the related spectroscopic data are reported below. All reagents and solvents were of analytical grade and were purchased from Sigma-Aldrich (Milano, Italy) or from Fluorochem (Hadfield, UK). Column chromatographies were performed on silica gel (Merck; 63–200 µm particle size). ¹H NMR and ¹³C NMR spectra were acquired at 25 °C, unless otherwise specified, on a Bruker AVANCE-400 spectrometer at 9.4 T (Bruker, Billerica, MA, USA), operating at 400 MHz (¹H NMR) and 100 MHz (¹³C-NMR); chemical shift values (δ) are given in ppm relative to TMS, using the solvent as the internal reference, while coupling constants are given in Hz. The following abbreviations were used: s = singlet, d = doublet, t = triplet, dd = double doublet, dt = double triplet, and m = multiplet. Mass spectra were recorded on a ThermoFinnigan (San Jose, CA, USA) LCQ Classic LC/MS/MS ion trap, equipped with an ESI source and a syringe pump;

samples (10^{-4} – 10^{-5} M in MeOH/H₂O 80:20) were infused in the electrospray system at a flow rate of 5–10 μLmin^{-1} ; when necessary, 50 μL of 10^{-2} M HCOOH was added to the sample solutions to promote analyte ionization; the ESI-MS data are given as m/z , with mass expressed in amu. Melting points were determined on a FALC Mod. 360 D (Falc Instruments, Treviglio, Italy) or on a Kofler apparatus and are uncorrected. Infrared spectra were recorded on a PerkinElmer (Waltham, MA, USA) Spectrum One FT-IR spectrometer in a nujol mull. The purity of the compounds was determined by elemental analyses, obtained by a PE 2400 (PerkinElmer, Waltham, MA, USA) analyzer, and the analytical results were within $\pm 0.4\%$ of the theoretical values for all compounds.

2.1.1. General Procedure for the Synthesis of Compounds

N-(3-(1*H*-imidazol-1-yl)propyl)-5-nitrofur-2-carboxamide (**2**) and 5-nitro-*N*-(2-(pyridin-2-yl)ethyl)furan-2-carboxamide (**3**)

As reported in Scheme 1, the 5-nitrofuran-2-carboxylic acid was added to a suspension of 1,1-carbonyldiimidazole (CDI) in 1,4-dioxane in a 1:1 molar ratio, and the reaction mixture was stirred at rT for 2 h. Then, the opportune amine (1 eq) was added, and the mixture was stirred at rT for 12 h and refluxed for an additional 2 h. After this time had passed, the reaction mixture was treated with 2 mL of H₂O and refluxed for 1 h. The solvent was removed under reduced pressure and the residue was treated with CH₂Cl₂ (10 mL) and NaOH (10 mL, 1 N). The organic phase was separated and washed with 10 mL of H₂O, dried over anhydrous Na₂SO₄, then filtered and concentrated in a vacuum. The obtained residue was subjected to silica gel column chromatography using AcOEt/MeOH as an eluent to afford the purified amide compounds **2** and **3**.



Scheme 1. Reagents and conditions: (a) CDI, 1,4-dioxane; (b) RNH₂.

N-(3-(1*H*-imidazol-1-yl)propyl)-5-nitrofuran-2-carboxamide (**2**)

Compound **2** was prepared using 5-nitrofuran-2-carboxylic acid (785 mg, 5 mmol), CDI (811 mg, 5 mmol) and 3-(1*H*-imidazol-1-yl)propan-1-amine (597 μL , $d = 1.049$ g/mL, 5 mmol) in 25 mL of 1,4-dioxane, following the general procedure. Compound **2** was obtained with 7% yield; $R_f = 0.59$ (AcOEt/MeOH 9:1). mp: 144–148 °C (Kofler). ESI-MS (m/z): 265.4 [M + H]⁺. Anal. (C₁₁H₁₂N₄O₄) C, H, N; calcd: C 50.00%, H 4.58%, N 21.20%; found: C 50.08%, H 4.58%, N 21.18%. IR (nujol mull, cm^{-1}): 3107; 1657; 1587; 1464; 1284. ¹H-NMR (MeOD) δ (ppm): 7.71 (s, 1H); 7.55 (d, 1H, $J = 3.6$ Hz); 7.30 (d, 1H, $J = 3.6$ Hz); 7.19 (s, 1H); 6.98 (s, 1H); 4.13 (t, 2H, $J = 6.8$ Hz); 3.42 (t, 2H, $J = 6.8$ Hz); 2.12 (m, 2H). ¹³C-NMR (MeOD) δ (ppm): 157.5; 151.8; 147.9; 137.1; 127.7; 119.2; 115.5; 111.9; 44.2; 36.3; 30.4 (Figures S1–S3).

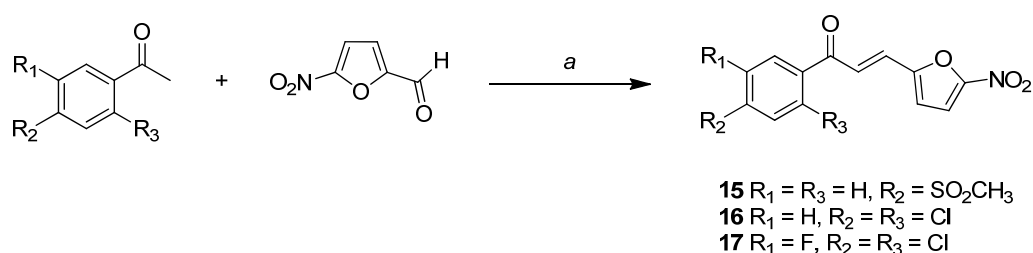
5-nitro-*N*-(2-(pyridin-2-yl)ethyl)furan-2-carboxamide (**3**)

Compound **3** was prepared using 5-nitrofuran-2-carboxylic acid (204 mg, 1.3 mmol), CDI (211 mg, 1.3 mmol) and 2-(pyridin-2-yl)ethanamine (156 μL , $d = 1.021$ g/mL, 1.3 mmol) in 9 mL of 1,4-dioxane, following the general procedure. Compound **3** was obtained with 30% yield. mp: 52–54 °C (Kofler). ESI-MS (m/z): 265.4 [M + H]⁺. Anal. (C₁₂H₁₁N₃O₄) C, H, N; calcd: C 55.17%, H 4.24%, N 16.09%; found: C 55.23%, H 4.25%, N 16.06%. IR (nujol mull, cm^{-1}): 3297; 1653; 1583; 1465; 1299. ¹H-NMR (MeOD) δ (ppm): 8.48 (d, 1H, $J = 4.8$ Hz); 7.77 (dt, 1H, $J = 1.8$ Hz, 7.8 Hz); 7.52 (d, 1H, $J = 3.8$ Hz); 7.37 (d, 1H, $J = 7.6$ Hz);

7.26–7.31 (m, 2H); 3.75 (t, 2H, $J = 7.2$ Hz); 3.10 (t, 2H, $J = 7.2$ Hz). $^{13}\text{C-NMR}$ (MeOD) δ (ppm): 158.6; 148.5; 148.0; 147.3; 143.1; 137.4; 123.7; 121.9; 115.3; 111.8; 39.1; 36.7 (Figures S4–S6).

2.1.2. General Procedure for the Synthesis of Compounds (*E*)-1-(4-(methylsulfonyl)phenyl)-3-(5-nitrofuran-2-yl)prop-2-en-1-one (**15**), (*E*)-1-(2,4-dichlorophenyl)-3-(5-nitrofuran-2-yl)prop-2-en-1-one (**16**) and (*E*)-1-(2,4-dichloro-5-fluorophenyl)-3-(5-nitrofuran-2-yl)prop-2-en-1-one (**17**)

The 5-nitrofuran-2-carbaldehyde and the opportune acetophenone, in a 1:1 molar ratio, were dissolved in 1.68 mL of acetic acid and sulfuric acid (67 μL , 98%) was added to the solution. The reaction mixture was stirred at 100 $^{\circ}\text{C}$ for 24 h (Scheme 2). After this time, the mixture was extracted with CH_2Cl_2 (3 \times 25 mL). The organic phase was dried over anhydrous Na_2SO_4 , filtered, and concentrated in a vacuum. The obtained residue was subjected to silica gel column chromatography to afford the purified compounds **15–17**.



Scheme 2. Reagents and conditions: (a) H_2SO_4 , CH_3COOH , 100 $^{\circ}\text{C}$, 24 h.

(*E*)-1-(4-(methylsulfonyl)phenyl)-3-(5-nitrofuran-2-yl)prop-2-en-1-one (**15**)

Compound **15** was prepared using 5-nitrofuran-2-carbaldehyde (105 μL , $d = 1.349$ g/mL, 1 mmol) and 1-(4-(methylsulfonyl)phenyl)ethanone (198 mg, 1 mmol), following the general procedure. Compound **15** was obtained as a yellow solid with 75% yield; $R_f = 0.59$ ($\text{CH}_2\text{Cl}_2/\text{AcOEt}$ 9.5:0.5). mp: 197–200 $^{\circ}\text{C}$ (dec). ESI-MS (m/z): 322.1 [$\text{M} + \text{H}$] $^+$. Anal. ($\text{C}_{14}\text{H}_{11}\text{NO}_6\text{S}$) C, H, N; calcd: C 52.33%, H 3.45%, N 4.36%; found: C 52.24%, H 3.44%, N 4.37%. IR (nujol mull, cm^{-1}): 3127; 3096; 1664; 1608; 1561; 1465; 1346. $^1\text{H-NMR}$ ($\text{DMSO-}d_6$) δ (ppm): 8.32 (d, 2H, $J = 7.9$ Hz); 8.12 (d, 2H, $J = 7.8$ Hz); 7.89–7.81 (m, 2H); 0.64 (d, 1H, $J = 15.7$ Hz); 7.47 (d, 1H, $J = 3.9$ Hz); 3.30 (s, 3H). $^{13}\text{C-NMR}$ ($\text{DMSO-}d_6$) δ (ppm): 188.4; 153.4; 152.6; 145.0; 141.0; 130.4; 129.9; 128.0; 125.2; 118.9; 115.2; 43.7 (Figures S7–S9).

(*E*)-1-(2,4-dichlorophenyl)-3-(5-nitrofuran-2-yl)prop-2-en-1-one (**16**)

Compound **16** was prepared using 5-nitrofuran-2-carbaldehyde (105 μL , $d = 1.349$ g/mL, 1 mmol) and 1-(2,4-dichlorophenyl)ethanone (189 mg, 1 mmol), following the general procedure. Compound **16** was obtained as a yellow solid with 17% yield; $R_f = 0.64$ ($\text{CH}_2\text{Cl}_2/\text{AcOEt}$ 9.5:0.5). mp: 164–165 $^{\circ}\text{C}$. Anal. ($\text{C}_{13}\text{H}_7\text{Cl}_2\text{NO}_4$) C, H, N; calcd: C 50.03%, H 2.26%, N 4.49%; found: C 50.18%, H 2.26%, N 4.50%. IR (nujol mull, cm^{-1}): 3107; 1657; 1587; 1548; 1464; 1284. $^1\text{H-NMR}$ (Acetone- d_6) δ (ppm): 7.67–7.64 (m, 2H); 7.61 (d, 1H, $J = 4.0$ Hz); 7.56 (dd, 1H, $J = 2.0$ Hz, $J = 8.4$ Hz); 7.44 (d, 1H, $J = 16.0$ Hz); 7.29–7.25 (m, 2H). $^{13}\text{C-NMR}$ (Acetone- d_6) δ (ppm): 190.7; 152.8; 152.5; 137.0; 136.8; 132.0; 131.0; 130.0; 129.9; 128.1; 127.7; 118.0; 113.5 (Figures S10–S12).

(*E*)-1-(2,4-dichloro-5-fluorophenyl)-3-(5-nitrofuran-2-yl)prop-2-en-1-one (**17**)

Compound **17** was prepared using 5-nitrofuran-2-carbaldehyde (105 μL , $d = 1.349$ g/mL, 1 mmol) and 1-(2,4-dichloro-5-fluorophenyl)ethanone (145 μL , $d = 1.425$ g/mL, 1 mmol), following the general procedure. Compound **17** was obtained as a yellow solid with 30% yield; $R_f = 0.52$ ($\text{CH}_2\text{Cl}_2/\text{Hexane}$ 7:3). mp: 163–165 $^{\circ}\text{C}$. Anal. ($\text{C}_{13}\text{H}_6\text{Cl}_2\text{FNO}_4$) C, H, N Calcd: C 47.30%, H 1.83%, N 4.24%; Found: C 48.01%, H 1.83%, N 4.25%. IR (nujol mull, cm^{-1}): 3089; 3070; 1660; 1612; 1463; 1346. $^1\text{H-NMR}$ ($\text{DMSO-}d_6$) δ (ppm): 8.01 (d, 1H, $J = 6.4$ Hz); 7.83–7.79 (m, 2H); 7.46–7.40 (m, 2H); 7.17 (d, 1H, $J = 16.0$ Hz). $^{13}\text{C-NMR}$ ($\text{DMSO-}d_6$) δ (ppm): 190.3; 156.1 (d, $J = 249.2$ Hz); 152.4; 152.2; 137.8 (d, $J = 6.1$ Hz); 131.9;

131.6; 127.8; 126.1 (d, $J = 3.7$ Hz); 122.9 (d, $J = 19.0$ Hz); 119.0; 117.7 (d, $J = 24.3$ Hz); 114.6 (Figures S13–S15).

2.2. Antifungal Drugs and Nitrofurans Derivatives

The antifungal drugs amphotericin B (AmB) and terbinafine (TRB) were purchased commercially (Sigma-Aldrich, Milano, Italy).

The nitrofurans derivatives were solubilized in 100% dimethyl sulfoxide (DMSO) at a stock concentration of 30,000 $\mu\text{g}/\text{mL}$ and were stored at -80 °C. Antifungal drugs stock solutions were prepared considering their purity, using the calculations recommended in document M27-A3. The working solutions of the compounds (0.06–250 $\mu\text{g}/\text{mL}$) and the drugs AmB (Sigma-Aldrich, Milano, Italy) (0.007–4 $\mu\text{g}/\text{mL}$) and TRB (Sigma-Aldrich, Milano, Italy) (0.001–1 $\mu\text{g}/\text{mL}$) were prepared in Roswell Park Memorial Institute (RPMI)-1640 medium with L-glutamine, without sodium bicarbonate, and with phenol red as the pH indicator (Gibco® Thermo-Fisher-Scientific, Waltham, MA, USA), buffered with 4-morpholinepropanesulfonic acid hemisodium salt (MOPS) (Sigma-Aldrich, Milano, Italy) with 2% glucose (Synth, Diadema, São Paulo, Brazil) pH = 7.

2.3. Microorganisms and Culture Conditions

The following fungi (strains) were used: *Candida albicans* (ATCC 90028); *C. krusei* (ATCC 6258); *C. glabrata* (ATCC 90030); *Cryptococcus neoformans* (H99/ATCC 208821); *Histoplasma capsulatum* (G217-B/ATCC 26032), *Paracoccidioides brasiliensis* (Pb 18), originally isolated from a case of pulmonary paracoccidioidomycosis in São Paulo, SP, Brazil [57], *Trichophyton mentagrophytes* (ATCC 11481), and *T. rubrum* (ATCC 28289). The strains of *Candida* and *Cryptococcus* were subcultured on Sabouraud dextrose agar (BD Difco™, Wokingham, Berkshire, UK) for 24 and 48 h, respectively, as described in document M27-A3 of the Clinical Institute Standards Laboratory (CLSI, Wayne, PA, USA) [58]. For *H. capsulatum*, the yeast phase of each strain was maintained in Brain and Heart Infusion (BHI) agar (BD Difco™, Wokingham, Berkshire, UK), supplemented with 0.1% L-cysteine (Synth, Diadema, São Paulo, Brazil) and 1% glucose (Sigma-Aldrich, Milano, Italy) for 96 h at 37 °C. The strains were subsequently subcultured in Ham's F-12 Nutrient Mixture medium (HAM-F12) (Gibco®-Thermo-Fisher-Scientific, Waltham, MA, USA) supplemented with 1.8% glucose (Synth, Diadema, São Paulo, Brazil), 0.1% glutamic acid (Synth, Diadema, São Paulo, Brazil), 0.6% HEPES (Sigma-Aldrich, Milano, Italy) and 0.0008% L-cysteine (Synth, Diadema, São Paulo, Brazil) at 37 °C, for 96 h and with shaking at 150 rpm [59,60]. *P. brasiliensis* was kept in Fava-Netto medium at 37 °C for 96 h [61]. The strains of *Trichophyton* were kept in malt extract agar (malt extract (Kasvi, São José do Pinhais, Paraná, Brazil): 2%; peptone from animal tissue (Sigma-Aldrich, Milano, Italy): 2%; glucose (Synth, Diadema, São Paulo, Brazil): 2%; agar (Kasvi, São José do Pinhais, Paraná, Brazil: 2%), pH 5.7, and incubated at 28 °C for 7 days or until sporulation [35,38].

2.4. Fungal Susceptibility to Nitrofurans Derivatives and Antifungal Drugs

2.4.1. *Candida* sp. and *Cryptococcus neoformans*

The susceptibility test for *Candida* and *C. neoformans* species was conducted as recommended in CLSI M27-A3 [58]; yeasts were adjusted at a concentration of 5×10^6 cells/mL, then a dilution of 1:50 was performed using 0.85% NaCl and 1:20 using RPMI-1640 medium (Gibco® -Thermo-Fisher-Scientific, Waltham, MA, USA). Dilutions of the compounds and antifungal reference drugs were dispensed in a 96-well microplate (Kasvi, São José do Pinhais, Paraná, Brazil) at a total volume of 100 $\mu\text{L}/\text{well}$; subsequently, 100 $\mu\text{L}/\text{well}$ of the inoculum was added and the plates were incubated at 37 °C for 24 h (*Candida* sp.) and 48 h (*C. neoformans*). A visual and colorimetric readout was performed with 0.03% resazurin (Sigma-Aldrich, Milano, Italy) [38,61,62]. Quality control was performed with *C. krusei* ATCC 6258 strains, using the drug AmB. MIC was considered when inhibition was at least 90% of the growth when compared to the control (MIC₉₀).

2.4.2. *Histoplasma capsulatum*

Susceptibility assays for *H. capsulatum* were performed according to the document M27-A3, proposed by CLSI [58], with modifications as proposed by Li and collaborators [63], Wheat and collaborators [64], and Kathuria and collaborators [65]. The inoculum was prepared in 0.85% NaCl, then the cell viability was checked with a hemocytometer using Trypan blue (Gibco® Thermo-Fisher-Scientific, Waltham, MA, USA) in a 1:1 ratio. The fungal suspension yeasts were adjusted at a 5×10^6 cells/mL concentration in 0.85% NaCl. Then, 1:10 dilution was performed and the fungal suspensions were placed in contact with the serial dilutions of the compounds and reference drug. The final fungal concentration was 2.5×10^5 cells/mL. The plates were incubated for 144 h at 37 °C while shaking at 150 rpm. Visual and colorimetric readings were performed by adding 30 µL of 0.03% resazurin.

2.4.3. *Paracoccidioides brasiliensis*

The susceptibility was conducted as described by de Paula e Silva et al. [61]; fungal suspensions were prepared at a 5×10^6 cells/mL concentration, diluted to 1:50 in 0.85% NaCl and 1:20 in RPMI-1640 medium. Serial dilution of the compounds was carried out and the result was placed in contact with the fungal suspension. The plates were incubated at 37 °C for 48 h at 150 rpm, and 20 µL of Alamar Blue (Invitrogen- Thermo-Fisher-Scientific, Waltham, MA, USA) was added and incubated for another 24 h for colorimetric readings.

2.4.4. *Trichophyton rubrum* and *T. mentagrophytes*

The experiments were performed according to CLSI M38-A2 [65] for dermatophytes, with minor modifications as described by Costa-Orlandi et al. [35]. The fungal suspensions were adjusted by counting the conidia in the hemocytometer to reach a final concentration of 2.5×10^3 cells/mL in RPMI-1640 medium. This was added to the wells at the appropriate compound concentrations and incubated at 35 °C for 96 h with agitation (150 rpm). Visual and colorimetric readings were taken with the addition of 20 µL of 0.03% resazurin [61]. Quality control was performed using the strain of *T. rubrum* ATCC MYA-4438, with the drug TRB.

2.5. Determination of Minimum Fungicide Concentration (MFC)

The minimum fungicidal concentration was performed as described by Costa-Orlandi et al. [35]. To be precise, 100 µL aliquots of the contents of the wells were removed and plated in specific media for each fungus. *Candida* spp. and *C. neoformans* were plated on Sabouraud dextrose agar (BD Difco™) and incubated at 37 °C for 24 h and 48 h, respectively. *H. capsulatum* was plated on BHI agar supplemented with 0.1% L-cysteine and 1% glucose and was subsequently incubated at 37 °C for 96 h; *P. brasiliensis* was plated on Fava-Neto medium at 37 °C for 72 h and dermatophytes on Sabouraud agar at 28 °C for 96 h. Concentrations greater than or equal to MIC₉₀ were used. The minimum fungicidal concentration is the lowest concentration of the compound or drug where the development of 99.9% of microorganisms does not occur [35].

2.6. Cell Line Maintenance

Two cell lines were used: the A549 (ATCC® CCL-185) lung epithelial cell line and the MRC-5 (ATCC® CCL-171) pulmonary fibroblast cell line. Both were grown in Dulbecco's Modified Eagle's Medium (DMEM) (Gibco), supplemented with 10% fetal bovine serum (FBS) (Sigma-Aldrich, Milano, Italy), and incubated in 5% CO₂ at 37 °C [66]. After thawing, the cell lines were expanded to reach 80% confluence, ready to be trypsinized and transferred to another bottle.

Cytotoxicity Assay in Monolayer Models by Resazurin Colorimetric Method

Cytotoxicity tests were performed for both strains (A549 and MRC-5) to verify the selectivity index (SI). The assay was performed as described by Costa-Orlandi et al. [35]

and Bila et al. [38]. Cell suspensions were prepared to obtain a final concentration of 2×10^4 cells/well in a 96-well microdilution plate. After 24 h of incubation, the culture medium was removed, and 200 μ L of different concentrations of nitrofurans were added. All the plates were incubated for 72 h. After incubation, 20 μ L of resazurin (Sigma-Aldrich, Milano, Italy) at 60 μ M was added, and the plates were further incubated for 8 h. Cell viability was assessed based on spectrophotometric analysis (Epoch, Biotek, Santa Clara, CA, USA) at wavelengths of 570 nm and 600 nm [67]. The SI was calculated according to the ratio between the IC_{50} and the MIC_{90} [68].

2.7. Toxicity In Vivo on *C. elegans* Model

The experiments were carried out with the mutant strain (AU37 [glp-4 (bn2) I; sek-1 (km4) X]). The strain was maintained on plates containing nematode growth medium (NGM) seeded with *Escherichia coli* OP50 at 16 °C. The stage of synchronization of young adults at stage L4 was performed for the toxicity test. About 20 larvae were transferred to each well of 96-well plates containing 100 μ L of a medium composed of 60% of 50 mM NaCl; 40% BHI broth; 10 mg/mL cholesterol in ethanol; 200 mg/mL ampicillin and 90 mg/mL kanamycin. Then, 100 μ L of dilutions of nitrofurans derivatives (showing the best selectivity index against the fungal species) were added. Final concentrations in each well ranged from 250 to 31.25 μ g/mL. Plates were incubated at 25 °C for 24 h. Survival was assessed by the mobility and shape of the nematode (stick-shaped larvae were considered dead, while sinusoidal larvae were considered alive) under an inverted optical microscope on 40 \times objective lenses [35,69–71].

2.8. Statistic Analysis

All tests were carried out in triplicate and in three independent experiments. Data were subjected to statistical analysis using an analysis of variance (one-way ANOVA) with a Bonferroni post-test, using GraphPad Prism 5.0 software (GraphPad Software Inc., La Jolla, CA, USA). All *p* values of less than 0.05 were considered statistically significant.

3. Results

3.1. Chemical Synthesis

The synthesis of 5-nitrofurans derivatives **2** and **3** involves the activation of the 5-nitro-furan-2 carboxylic acid with carbonyl-diimidazole (CDI) and the subsequent reaction with the appropriate amine. The obtained amide derivatives were purified by silica gel column chromatography and characterized by MS-ESI spectrometry, IR, 1H and ^{13}C -NMR spectroscopy; the analytical data were in accordance with the proposed structures. Specifically, in addition to the expected molecular peaks in the ESI-MS spectra, the shifts of the methylene signals, from 2.6 to 3.4 ppm for compound **2** and from about 2.9 to 3.7 ppm for compound **3** due to the transformation from primary amine to amide, are diagnostic. Furthermore, the presence of carbonyl stretching at 1657 cm^{-1} and 1650 cm^{-1} for **2** and **3**, respectively, indicate the extension of conjugation and further confirm the proposed structures.

For the synthesis of nitrofurans **15–17**, the 5-nitrofurans-2-carbaldehyde reacted with the opportune acetophenone in the presence of sulfuric and acetic acid. The obtained chalcones were purified by silica gel column chromatography and characterized by spectroscopic techniques. In particular, the low-frequency shift of the carbonyl stretching signal observed in the chalcones, compared to the corresponding acetophenones, supports the double-bond formation (1664 vs. 1685 cm^{-1} for **15**, 1677 vs. 1698 cm^{-1} for **16**, and 1660 vs. 1707 cm^{-1} for **17**); these data are confirmed by ^{13}C -NMR spectra, which show the presence of vinyl carbons. The expected E geometry of the double bond is confirmed by the typical 3J values of approximately 16 Hz of the trans vinyl coupling constant observed in the 1H -NMR spectra of compounds **15–17**.

3.2. Broad-Spectrum Antifungal Activity

In general, yeasts were resistant to most compounds with a prevalence of MIC₉₀ greater than or equal to 250 µg/mL in 72% of the compounds against *Candida* species and 47% against *C. neoformans* (Figure 2). *H. capsulatum* (41%), *P. brasiliensis* (47%), and dermatophytes (35%) were more sensitive to nitrofurans, with a prevalent MIC₉₀ of 7.81–1.95 µg/mL (Figure 2). In addition, *P. brasiliensis* was particularly sensitive to the tested compounds; indeed, all nitrofurans tested against *P. brasiliensis* had an MIC₉₀ of between 31.25 and 0.48 µg/mL (Figure 2).

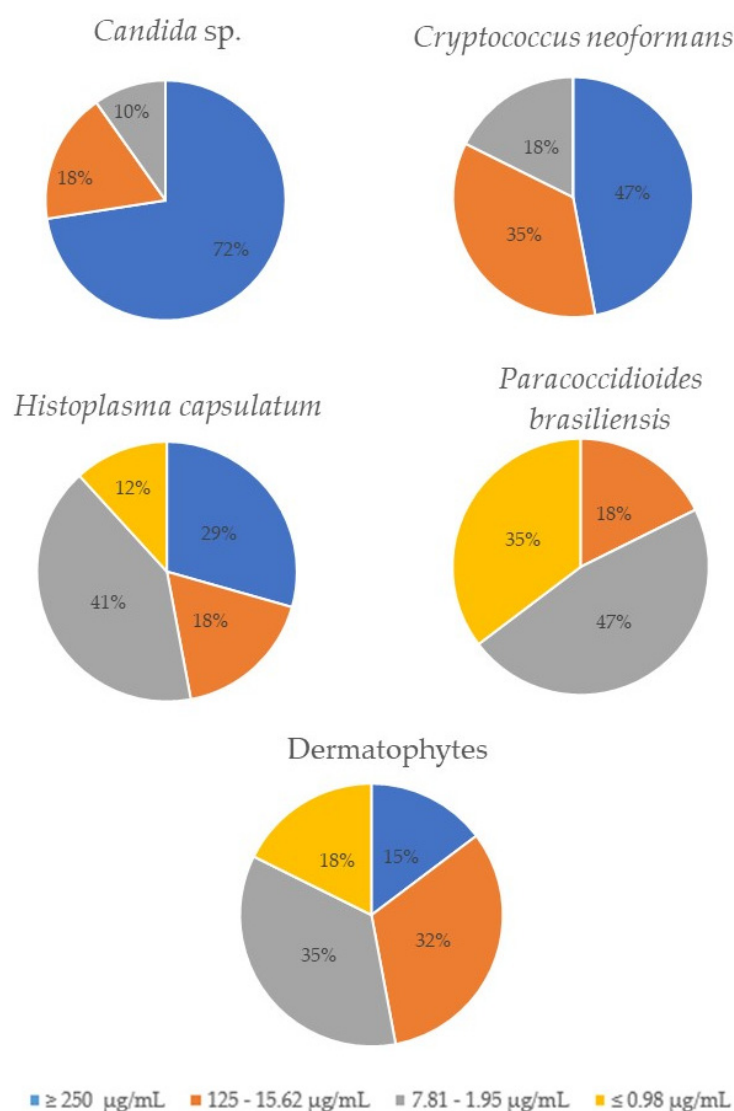


Figure 2. Representative graphs of the MIC₉₀ obtained for each fungal species, for the 17 tested nitrofuran derivatives.

3.3. Determination of MIC₉₀ and MFC for *Candida* species and *Cryptococcus neoformans*

For *Candida* species, the MIC₉₀ ranged from 3.9 to values higher than 250 µg/mL (Table 1). Most compounds showed a fungicidal profile with MFC values from 7.81 to greater than 250 µg/mL (Table 1). For *Cryptococcus neoformans*, the MIC₉₀ of nitrofuran derivatives also ranged from 3.9 to greater than 250 µg/mL, with a fully fungicidal profile, the MFC being equal to or two times greater than the MIC₉₀ (Table 1). The susceptibility test results for the strain of *C. krusei* with AmB gave an MIC₉₀ of 1 µg/mL, proving the quality of the experiments.

Table 1. Minimum inhibitory and fungicidal concentration values ($\mu\text{g}/\text{mL}$) of the 17 nitrofurane derivatives against *C. albicans*, *C. krusei*, *C. glabrata*, and *Cryptococcus neoformans*.

Compounds	<i>C. albicans</i>		<i>C. krusei</i>		<i>C. glabrata</i>		<i>C. neoformans</i>	
	MIC ₉₀	MFC	MIC ₉₀	MFC	MIC ₉₀	MFC	MIC ₉₀	MFC
1	3.90	125.00	31.25	31.25	7.81	>250	31.25	31.25
2	>250	>250	>250	>250	>250	>250	\geq 250	\geq 250
3	>250	>250	250.00	>250	>250	>250	31.25	62.50
4	250.00	>250	250.00	250.00	>250	>250	31.25	62.50
5	125.00	250.00	62.50	62.50	125.00	125.00	7.81	15.62
6	>250	>250	>250	>250	>250	>250	250.00	250.00
7	250.00	>250	250.00	>250	>250	>250	62.5	62.5
8	7.80	>250	250.00	>250	7.81	>250	31.25	31.25
9	15.62	31.25	250.00	>250	31.25	>250	7.81	15.62
10	250.00	>250	>250	>250	>250	>250	250.00	\geq 250
11	125.00	250.00	250.00	>250	250.00	>250	\geq 250	\geq 250
12	250.00	>250	250.00	>250	250.00	>250	62.50	125.00
13	>250	>250	>250	>250	>250	>250	\geq 250	\geq 250
14	15.60	62.50	15.60	31.25	7.81	7.81	3.90	3.90
15	>250	>250	>250	>250	>250	>250	\geq 250	\geq 250
16	250.00	>250	>250	>250	>250	>250	\geq 250	\geq 250
17	>250	>250	>250	>250	>250	>250	\geq 250	\geq 250
AmB	-	-	1	-	-	-	0.06	-

MIC₉₀—minimum inhibitory concentration capable of inhibiting at least 90% growth; MFC—minimal fungicidal concentration; AmB: Amphotericin B.

3.4. Determination of MIC and MFC for *H. capsulatum* and *P. brasiliensis*

The MIC₉₀ scores ranged from 0.48 to over 250 $\mu\text{g}/\text{mL}$ for the *H. capsulatum* strain and from 0.48 to 31.25 $\mu\text{g}/\text{mL}$ for *P. brasiliensis* (Table 2). Compound 1 showed a fungistatic profile when tested against the *P. brasiliensis* strain; otherwise, the other active compounds showed a fungicidal profile for both fungi. AmB showed an MIC₉₀ of 0.03 $\mu\text{g}/\text{mL}$ for *H. capsulatum* and 0.13 $\mu\text{g}/\text{mL}$ for *P. brasiliensis*.

Table 2. Minimum inhibitory and fungicidal concentration values ($\mu\text{g}/\text{mL}$) of the 17 nitrofurane derivatives against *H. capsulatum* and *P. brasiliensis*.

Compounds	<i>H. capsulatum</i>		<i>P. brasiliensis</i>	
	MIC ₉₀	MFC	MIC ₉₀	MFC
1	>250	>250	3.90	62.50
2	250.00	>250	31.25	125.00
3	3.90	3.90	0.48	0.98
4	3.90	3.90	3.90	7.81
5	1.95	1.95	15.62	31.25
6	>250	>250	31.25	31.25
7	0.98	0.98	1.95	1.95
8	15.62	15.62	0.98	1.95
9	3.90	3.90	0.48	1.95
10	7.81	15.62	0.98	0.98
11	0.48	0.48	0.98	0.98
12	7.81	15.62	3.90	3.90
13	125.00	125.00	0.98	0.98
14	7.81	7.81	1.95	1.95
15	>250	>250	3.90	7.81
16	62.50	62.50	1.95	1.95
17	>250	>250	1.95	3.90
AmB	0.03	-	0.13	-

MIC₉₀—minimum inhibitory concentration capable of inhibiting at least 90% growth; MFC—minimal fungicidal concentration; AmB: Amphotericin B.

3.5. Determination of MIC and MFC for *T. mentagrophytes*

For both *T. rubrum* and *T. mentagrophytes* dermatophyte strains, the MIC₉₀ ranged from 0.98 to greater than 250 µg/mL (Table 3). Compounds **3** and **4** showed a fungistatic profile on *T. mentagrophytes*, while **16** showed a fungistatic profile on *T. rubrum*. TRB showed a MIC₉₀ of 0.03 µg/mL to the control strain *T. rubrum* ATCCMYA-4438, proving the quality of the experiments.

Table 3. Minimum inhibitory and fungicidal concentration values (µg/mL) of the 17 nitrofurans derivatives against dermatophytes.

Compounds	<i>T. rubrum</i>		<i>T. mentagrophytes</i>		<i>T. rubrum</i> ATCC MYA-4438
	MIC ₉₀	MFC	MIC ₉₀	MFC	MIC ₉₀
1	>250	>250	15.60	15.60	-
2	125.00	>250	125.00	125.00	-
3	125.00	125.00	62.50	250.00	-
4	125.00	125.00	31.25	250.00	-
5	15.65	31.25	31.25	62.50	-
6	>250	>250	>250	>250	-
7	125.00	>250	125.00	>250	-
8	0.98	1.95	0.98	1.95	-
9	0.98	1.95	1.95	1.95	-
10	3.90	7.81	3.90	7.81	-
11	7.80	15.60	7.80	7.80	-
12	0.98	1.95	1.95	1.95	-
13	0.98	1.95	0.98	0.98	-
14	1.95	3.9	1.95	1.95	-
15	7.8	15.6	7.8	15.6	-
16	7.80	31.25	7.80	7.80	-
17	>250	>250	>250	>250	-
TRB					0.03

MIC₉₀—minimum inhibitory concentration capable of inhibiting at least 90% growth; MFC—minimal fungicidal concentration; TRB: terbinafine.

3.6. Cytotoxicity Assay by the Resazurin Method and Selectivity Index

The cytotoxicity assay was performed using the resazurin colorimetric method. After quantifying the viability, the compounds' inhibition index of 50% of cell proliferation (IC₅₀) was calculated. For the A549 cell line, the IC₅₀ ranged from 8.58 to 250 µg/mL (Table 4). The selectivity index (SI) ranged from 0.03 to 64.10 for *Candida* species, 0.04 to 8.57 for *C. neoformans*, 0.05 to 59.28 for *H. capsulatum*, 0.42 to 481.66 for *P. brasiliensis*, and 0.05 to 255.10 for dermatophytes. For the MRC-5 cell line, the IC₅₀ ranged from 1.56 to 250 µg/mL (Table 5). The SI ranged from 0.006 to 61.66 for *Candida* species, 0.006 to 10.19 for *C. neoformans*, 0.006 to 130.33 for *H. capsulatum*, 0.49 to 520.83 for *P. brasiliensis*, 0.006 to 232.65 for *T. rubrum*, and 0.006 to 116.92 for *T. mentagrophytes*.

3.7. Toxicity on *C. elegans* Model

According to the selectivity index results, compounds **1**, **3**, **5**, **11** and **12** were evaluated in vivo in *C. elegans*.

All compounds were tested on AU37 larvae, which showed a viability higher than 80%, even when treated with the highest concentration of the tested compounds (250 µg/mL). Compounds **1** and **12** caused less toxicity in the larvae, which maintained viability more significant than 94% at a concentration of 250 µg/mL (Figure 3). The larvae treated with compounds **3**, **5** and **11** showed a decrease in viability only at the highest concentration value (250 µg/mL) when compared to the control ($p < 0.01$; $p < 0.05$; $p < 0.001$, respectively) (Figure 3). The larvae images were obtained from the wells with the highest concentration

of compounds (250 µg/mL); as can be observed, there are few dead larvae (rod-shaped), and most of them are sinusoidal (alive) (Figure 4).

Table 4. Selectivity index (MIC₉₀/IC₅₀) of nitrofurans derivatives against different fungi species compared to an A549 lung cell.

Compounds	A549 IC ₅₀ (µg/mL)	Calculated SI							
		<i>C. albicans</i>	<i>C. krusei</i>	<i>C. glabrata</i>	<i>C. neoformans</i>	<i>H. capsulatum</i>	<i>P. brasiliensis</i>	<i>T. rubrum</i>	<i>T. mentagrophytes</i>
1	250	64.10	8.00	32.01	8.00	1.00	64.10	1.00	16.02
2	49.1	0.19	0.19	0.19	0.19	0.19	1.57	0.39	0.39
3	231.2	0.92	0.92	0.92	7.39	59.28	481.66	1.84	3.69
4	29.5	0.11	0.11	0.11	1.89	7.56	7.56	0.23	0.94
5	30.11	0.24	0.48	0.24	7.72	15.44	1.92	1.92	0.96
6	13.21	0.05	0.05	0.05	0.05	0.05	0.42	0.05	0.05
7	8.58	0.03	0.03	0.03	0.13	8.75	4.40	0.06	0.06
8	53.8	6.89	0.21	6.88	1.72	3.44	55.46	54.89	54.89
9	23.41	1.49	0.09	0.74	1.50	6.00	48.77	23.88	12.00
10	38.67	0.15	0.15	0.15	0.15	4.95	39.86	9.91	9.91
11	12.24	0.09	0.04	0.04	0.04	25.50	12.61	1.56	1.56
12	250	1.00	1.00	1.00	1.00	32.01	64.10	255.10	128.20
13	17.9	0.07	0.07	0.07	0.07	0.14	18.26	18.26	18.26
14	33.44	2.14	2.14	4.28	8.57	4.28	17.14	17.14	17.14
15	34.23	0.13	0.13	0.13	0.13	0.13	8.77	4.38	4.38
16	35.58	0.14	0.14	0.14	0.14	0.56	17.96	4.56	4.56
17	68.18	0.27	0.27	0.27	0.27	0.27	34.96	0.27	0.27

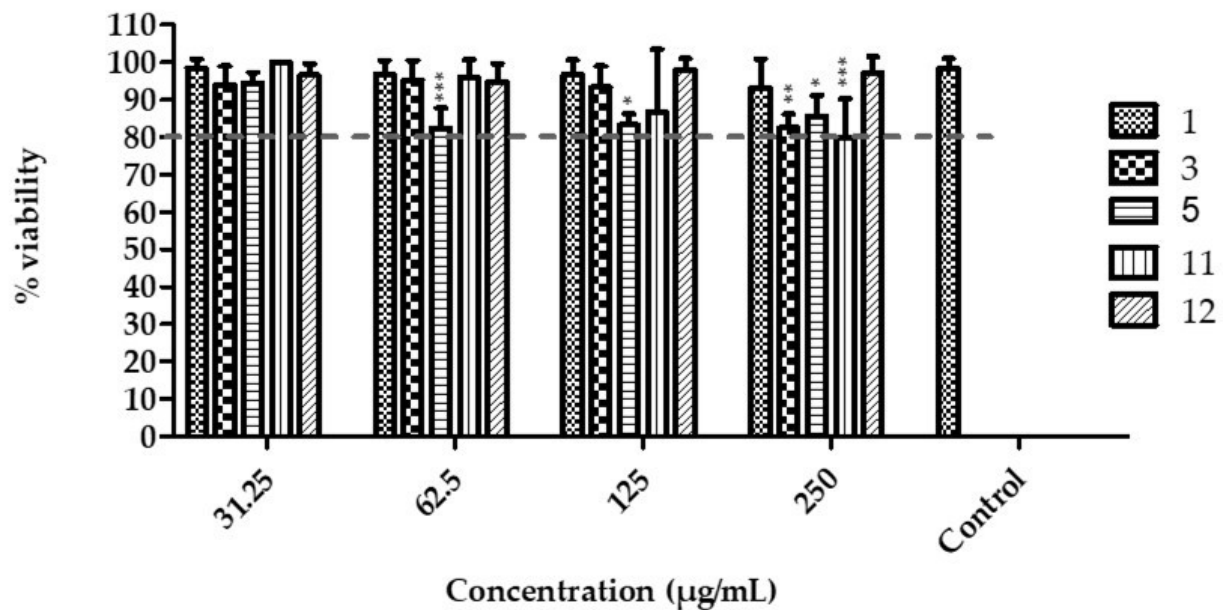
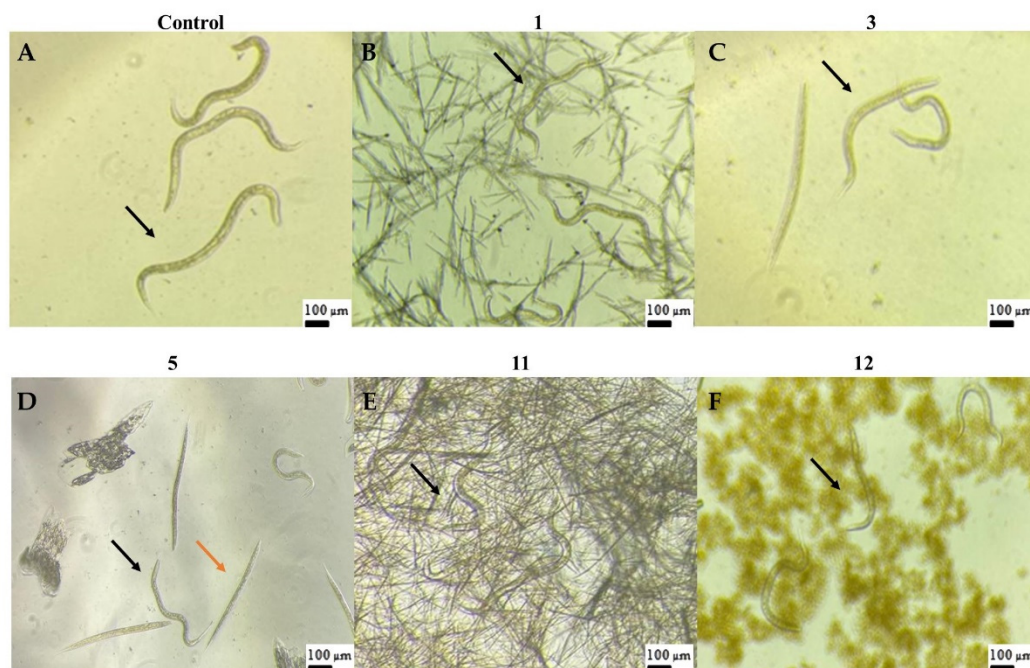


Figure 3. *Caenorhabditis elegans* larvae viability after treatment with the tested compounds. The larvae viability was greater than 80% with all the tested nitrofurans, even at the highest concentration of the compounds (250 µg/mL). The effects of the compounds were compared to the control group. Nitrofurans 1 and 12 showed no statistical difference with the control group in any concentration. On the other hand, compounds 3, 5 and 11, at the concentration of 250 µg/mL, showed statistical difference with the control group, with * $p < 0.01$, ** $p < 0.05$ and *** $p < 0.001$, respectively. Compound 5 also showed statistical difference with the control group at the concentrations of 125 µg/mL ($p < 0.05$) and 62.5 µg/mL ($p < 0.001$).

Table 5. Selectivity index (MIC_{90}/IC_{50}) of nitrofuran derivatives against different fungi species compared to the MRC-5 lung cells.

Compounds	MRC5 IC ₅₀ ($\mu\text{g/mL}$)	Calculated SI							
		<i>C. albicans</i>	<i>C. krusei</i>	<i>C. glabrata</i>	<i>C. neoformans</i>	<i>H. capsulatum</i>	<i>P. brasiliensis</i>	<i>T. rubrum</i>	<i>T. mentagrophytes</i>
1	240.5	61.66	7.69	30.79	7.69	0.96	61.66	0.96	15.41
2	90.75	0.36	0.36	0.36	0.36	0.36	2.90	0.72	0.72
3	250.00	1.00	1.00	1.00	8.00	64.10	520.83	2.00	4.00
4	135.2	0.54	0.54	0.54	8.66	34.66	34.66	1.08	4.32
5	39.76	0.31	0.63	0.31	10.19	20.38	2.54	2.54	1.27
6	15.6	0.06	0.06	0.06	0.06	0.06	0.49	0.06	0.06
7	71.24	0.28	0.28	0.28	1.13	72.69	36.53	0.56	0.56
8	6.66	0.85	0.02	0.85	0.21	0.42	6.86	6.79	6.79
9	47.23	3.02	0.18	1.51	3.02	12.11	98.39	48.19	24.22
10	215.4	0.86	0.86	0.86	0.86	27.58	222.06	55.23	55.23
11	62.56	0.50	0.25	0.25	0.25	130.33	64.49	8.02	8.02
12	228	0.91	0.91	0.91	0.91	29.19	58.46	232.65	116.92
13	4.15	0.01	0.01	0.01	0.01	0.03	4.23	4.23	4.23
14	26.8	1.71	1.71	3.43	6.87	3.43	13.74	13.74	13.74
15	11.51	0.04	0.04	0.04	0.04	0.04	2.95	1.47	1.47
16	29.89	0.11	0.11	0.11	0.11	0.47	15.09	3.83	3.83
17	1.56	0.006	0.006	0.006	0.006	0.006	0.80	0.006	0.006

**Figure 4.** Images of L4 stage *Caenorhabditis elegans*: 32 larvae at a compound concentration equal to 250 $\mu\text{g/mL}$. (A)—control group, the black arrow indicates a live larva, in its sinusoidal form; (B–F)—representative images of compounds 1, 3, 5, 11, and 12, respectively; the black arrows point to a live larva in its characteristic shape (sinusoidal) and the orange arrow shows a dead larva in its characteristic rod shape.

4. Discussion

Fungal diseases can affect the oral mucosa, skin, nails, hair, lungs, brain, or several organs and tissues simultaneously [6,18,19,24,25,35]. Constant global changes and the advent of new pandemics and chronic diseases favor the diffusion of fungal pathogens such as *Candida*, *Cryptococcus*, *Aspergillus*, *Trichophyton*, and dimorphic fungi such as *H. capsulatum* and *P. brasiliensis* [1,2,26].

Fungal diseases are often neglected, and the rapid and accurate identification of fungi in clinical practice is limited. Besides this, since some infections require a long period of drug intervention, not counting the high recurrence rates, treatments with antifungals can be costly in addition to their toxicity [1,72,73]. For this reason, the search for new effective

therapeutic alternatives for fungal infections is emerging, combined with research that minimizes the use of mammals.

We used cell cultures, which have become one of the most frequently applied techniques to replace or complement animal studies *in vivo*, helping in the toxicity and efficacy tests of new molecules [74,75]. In addition to cell cultures, non-mammalian alternative animals are widely used for pharmacological safety tests. *C. elegans* is classified as a nematode and measures about 1 mm in length, feeding on bacteria and fungi that decompose in the soil. It was characterized in the 1960s and has been essential in research, particularly in toxicology [76]. The AU37 strain has a *glp-4* mutation that makes the larvae incapable of reproducing at 25 °C, while the mutation in *sek-1* is responsible for making the larvae more sensitive to several pathogens [71,77].

One of the parameters used to verify the safety and potency of drugs or prototypes is the selectivity index. Values greater than ten are considered a sign of specificity and high selectivity [38,78,79]. Our findings show that nitrofurantoin **1** was the most promising among the tested compounds against *Candida* species, with MIC₉₀ values ranging from 3.9 to 31.25 µg/mL and a selectivity index ranging from 7.69 to 30.79. Similar results with nitrofurantoin derivatives were obtained by De Vita et al. [45,47], with MIC₅₀ values against *C. albicans* of between 0.5 and ≥128 µg/mL, and by Kamal et al. [46], with MIC values against *C. albicans* from 3.9 to 62.5 µg/mL. Furthermore, among the compounds tested on *C. elegans* larvae, compound **1** gave a viability percentage of 94% at a concentration of 250 µg/mL when we analyzed the acute toxicity of this compound, thus suggesting the low/null toxicity of this nitrofurantoin derivative.

Compound **5** showed higher potency against *C. neoformans* (MIC₉₀ 7.81 µg/mL and MFC 15.62 µg/mL), with SI from 7.72 to 10.19 on A549 and MRC5 cells, respectively. When the acute toxicity in *C. elegans* larvae was analyzed, this compound gave a viability of 85.65% at the highest concentration tested (250 µg/mL). Reports of antifungal resistance in *Cryptococcus* strains are increasing [80,81]. However, fluconazole-resistant isolates have been reported [82,83] and their emergence is thought to be due to the frequent use of the drug as a preventive of cryptococcal meningitis or asymptomatic cryptococcal antigenemia [82–84].

The most active compound to *H. capsulatum* was **11** (MIC₉₀ 0.48 µg/mL and MFC 0.48 µg/mL) with SI values of 25.50 and 130.33 on A549 and MRC5 cells, respectively. Otherwise, regarding *P. brasiliensis*, the most potent derivative was compound **3** (MIC₉₀ 0.48 µg/mL and MFC 0.98 µg/mL), with SI values of 481.66 to 520.83 on A549 and MRC5 cells, respectively. Concerning acute toxicity in *C. elegans* larvae, compound **11** gave 80% viability, and compound **3**, 82.48% at the highest concentration tested (250 µg/mL). These fungi cause systemic mycosis, and their treatment is limited and with high levels of toxicity [30,34,85]. These data indicate that nitrofurantoin derivatives have good antifungal properties (both fungistatic and fungicidal) toward these species; on the other hand, they also showed a good selectivity and low toxicity, both on cell lines and on larvae.

Compound **12** was the most potent and the most selective on dermatophyte strains, showing good fungicidal and fungistatic activity against *T. rubrum* (MIC₉₀ 0.98 µg/mL and MFC 1.95 µg/mL) and *T. mentagrophytes* (MIC₉₀ 1.95 µg/mL and MFC 1.95 µg/mL). Furthermore, this compound showed low toxicity *in vitro*, with SI values toward *T. rubrum* of 255.10 on A549 and 232.65 on MRC5 cells, respectively, and SI values toward *T. mentagrophytes* of 128.20 on A549 and 116.92 on MRC5 cells, respectively. In *C. elegans*, the viability was 97.20% at the highest concentration tested (250 µg/mL). Dermatophytes are filamentous fungi with a high prevalence in the human population [38,62] and usually cause infections that are difficult to eradicate and often recur [38,39].

Our results showed that some nitrofurantoin derivatives have broad-spectrum antifungal activity, with low toxicity and great potential to treat infections caused by these fungi.

Overall, this study yielded hopeful results as some of the derivatives studied showed low toxicity in both *in vitro* and *in vivo* tests, and, for the most part, presented a fungicidal profile.

5. Conclusions

On the whole, this study prompted us to identify new nitrofurans derivatives with a potent and broad-spectrum antifungal activity that is mainly due to fungicidal action; naturally, the values of the MIC and MFC as determined varied in a wide range but this variation is to be expected, as there are different fungal strains and species. It is noteworthy that the most potent antifungal nitrofurans, compounds **1**, **3**, **5**, **11**, and **12**, showed low toxicity, both in vitro on A549 and MRC5 cell cultures, showing high SI values, and in vivo on *C. elegans* larvae, showing a viability higher than 80% at the highest concentration tested. These results showed that nitrofurans derivatives are promising compounds for treating fungal infections with a broad spectrum. New studies will be carried out to investigate their effectiveness in communities of microorganisms and in vivo in other alternative animals, to elucidate their mechanism of action.

Supplementary Materials: The following supporting information can be downloaded at: <https://www.mdpi.com/article/10.3390/pharmaceutics14030593/s1>; it contains experimental details of chemical synthesis and spectroscopic data of some synthesized compounds. Table S1: list of CAS number of nitrofurans **4–14**; Figure S1: IR spectrum (nujol mull) of compound **2**; Figure S2: ¹H NMR spectrum (400 MHz, MeOD) of compound **2**; Figure S3: ¹³C NMR spectrum (100 MHz, MeOD) of compound **2**; Figure S4: IR spectrum (nujol mull) of compound **3**; Figure S5: ¹H NMR spectrum (400 MHz, MeOD) of compound **3**; Figure S6: ¹³C NMR spectrum (100 MHz, MeOD) of compound **3**; Figure S7: IR spectrum (nujol mull) of compound **15**; Figure S8: ¹H NMR spectrum (400 MHz, DMSO-*d*₆) of compound **15**; Figure S9: ¹³C NMR spectrum (100 MHz, DMSO-*d*₆) of compound **15**; Figure S10: IR spectrum (nujol mull) of compound **16**; Figure S11: ¹H NMR spectrum (400 MHz, Acetone-*d*₆) of compound **16**; Figure S12: ¹³C NMR spectrum (100 MHz, Acetone-*d*₆) of compound **16**; Figure S13: IR spectrum (nujol mull) of compound **17**; Figure S14: ¹H NMR spectrum (400 MHz, DMSO-*d*₆) of compound **17**; Figure S15: ¹³C NMR spectrum (100 MHz, DMSO-*d*₆) of compound **17**.

Author Contributions: Conceptualization, R.C., C.B.C.-O. and A.M.F.-A.; data curation, C.O.V., F.P., N.M.B., D.D.V., M.B. and V.T.; formal analysis, N.M.B., C.B.C.-O., A.M.F.-A. and L.S.; funding acquisition, M.J.S.M.-G., R.C. and L.S.; investigation, C.O.V., F.P., N.M.B., D.D.V., M.B., V.T. and C.B.C.-O.; methodology, C.O.V., F.P., N.M.B., D.D.V. and M.B.; project administration, M.J.S.M.-G. and A.M.F.-A.; resources, M.J.S.M.-G. and A.M.F.-A.; supervision, M.J.S.M.-G., A.M.F.-A. and L.S.; writing—original draft, C.O.V., F.P., N.M.B., D.D.V., M.B., V.T., C.B.C.-O., A.M.F.-A. and L.S.; writing—review and editing, M.B., M.J.S.M.-G., V.T., R.C., C.B.C.-O. and L.S. All authors have read and agreed to the published version of the manuscript.

Funding: This research was funded by the Fundação de Amparo à Pesquisa do Estado de São Paulo—FAPESP [Grants 2020/15586-4 (COV); 2019/22188-8 (NMB); 2017/18388-6 (CBC-O); 16/11836-0 (MJS-M-G)]; Programa de Apoio ao Desenvolvimento Científico (PADC) da Faculdade de Ciências Farmacêuticas da UNESP, Coordenação de Aperfeiçoamento de Pessoal de Nível Superior (CAPES) [Finance code 001; 88887.500765/2020-00 (COV)], Conselho Nacional de Desenvolvimento Científico e Tecnológico (CNPq) 134559/2018-5 (COV); 142049/2019-0 (NMB).

Institutional Review Board Statement: Not applicable.

Informed Consent Statement: Not applicable.

Data Availability Statement: Not applicable.

Acknowledgments: We thank Allan Jefferson Guimarães for kindly providing *H. capsulatum* G217-B/ATCC 26032 and Regina Helena Pires for the strains of *Candida*.

Conflicts of Interest: The authors declare no conflict of interest.

References

1. Bongomin, F.; Gago, S.; Oladele, R.O.; Denning, D.W. Global and Multi-National Prevalence of Fungal Diseases—Estimate Precision. *J. Fungi* **2017**, *3*, 57. [CrossRef]
2. Limper, A.H.; Adenis, A.; Le, T.; Harrison, T.S. Fungal infections in HIV/AIDS. *Lancet Infect. Dis.* **2017**, *17*, e334–e343. [CrossRef]
3. Basso, R.P.; Poester, V.R.; Benelli, J.L.; Stevens, D.A.; Zogbi, H.E.; da S. Vasconcellos, I.C.; Pasqualotto, A.C.; Xavier, M.O. COVID-19-Associated Histoplasmosis in an AIDS Patient. *Mycopathologia* **2021**, *186*, 109–112. [CrossRef]

4. Rawson, T.M.; Wilson, R.C.; Holmes, A. Understanding the role of bacterial and fungal infection in COVID-19. *Clin. Microbiol. Infect.* **2021**, *27*, 9–11. [[CrossRef](#)]
5. Song, G.; Liang, G.; Liu, W. Fungal Co-infections Associated with Global COVID-19 Pandemic: A Clinical and Diagnostic Perspective from China. *Mycopathologia* **2020**, *185*, 599–606. [[CrossRef](#)]
6. Ivaskiene, M.; Matusevicius, A.P.; Grigonis, A.; Zamokas, G.; Babickaite, L. Efficacy of Topical Therapy with Newly Developed Terbinafine and Econazole Formulations in the Treatment of Dermatophytosis in Cats. *Pol. J. Vet. Sci.* **2016**, *19*, 535–543. [[CrossRef](#)]
7. Arya, N.R.; Rafiq, N.B. Candidiasis. In *StatPearls*; StatPearls Publishing LLC: Treasure Island, FL, USA, 2021.
8. Garcia, L.M.; Costa-Orlandi, C.B.; Bila, N.M.; Vaso, C.O.; Gonçalves, L.N.C.; Fusco-Almeida, A.M.; Mendes-Giannini, M.J.S. A Two-Way Road: Antagonistic Interaction between Dual-Species Biofilms Formed by *Candida albicans*/*Candida parapsilosis* and *Trichophyton rubrum*. *Front. Microbiol.* **2020**, *11*, 1980. [[CrossRef](#)]
9. Sardi, J.C.O.; Scorzoni, L.; Bernardi, T.; Fusco-Almeida, A.M.; Mendes Giannini, M.J.S. *Candida* species: Current epidemiology, pathogenicity, biofilm formation, natural antifungal products and new therapeutic options. *J. Med. Microbiol.* **2013**, *62*, 10–24. [[CrossRef](#)]
10. Lee, Y.; Puumala, E.; Robbins, N.; Cowen, L.E. Antifungal Drug Resistance: Molecular Mechanisms in *Candida albicans* and Beyond. *Chem. Rev.* **2021**, *121*, 3390–3411. [[CrossRef](#)]
11. Paul, S.; Singh, S.; Sharma, D.; Chakrabarti, A.; Rudramurthy, S.M.; Ghosh, A.K. Dynamics of in vitro development of azole resistance in *Candida tropicalis*. *J. Glob. Antimicrob. Resist.* **2020**, *22*, 553–561. [[CrossRef](#)]
12. Espinel-Ingroff, A.; Cantón, E.; Pemán, J. Antifungal Resistance among Less Prevalent *Candida* Non-*albicans* and Other Yeasts versus Established and under Development Agents: A Literature Review. *J. Fungi* **2021**, *7*, 24. [[CrossRef](#)]
13. Campoy, S.; Adrio, J.L. Antifungals. *Biochem. Pharm.* **2017**, *133*, 86–96. [[CrossRef](#)]
14. Sanglard, D. Emerging Threats in Antifungal-Resistant Fungal Pathogens. *Front. Med.* **2016**, *3*, 11. [[CrossRef](#)]
15. Chang, Y.L.; Yu, S.J.; Heitman, J.; Wellington, M.; Chen, Y.L. New facets of antifungal therapy. *Virulence* **2017**, *8*, 222–236. [[CrossRef](#)]
16. Rajasingham, R.; Smith, R.M.; Park, B.J.; Jarvis, J.N.; Govender, N.P.; Chiller, T.M.; Denning, D.W.; Loyse, A.; Boulware, D.R. Global burden of disease of HIV-associated cryptococcal meningitis: An updated analysis. *Lancet Infect. Dis.* **2017**, *17*, 873–881. [[CrossRef](#)]
17. Hagen, F.; Khayhan, K.; Theelen, B.; Kolecka, A.; Polacheck, I.; Sionov, E.; Falk, R.; Parnmen, S.; Lumbsch, H.T.; Boekhout, T. Recognition of seven species in the *Cryptococcus gattii*/*Cryptococcus neoformans* species complex. *Fungal Genet. Biol.* **2015**, *78*, 16–48. [[CrossRef](#)]
18. Maziarz, E.K.; Perfect, J.R. Cryptococcosis. *Infect. Dis. Clin. N. Am.* **2016**, *30*, 179–206. [[CrossRef](#)]
19. Lee, H.H.; Del Pozzo, J.; Salamanca, S.A.; Hernandez, H.; Martinez, L.R. Reduced phagocytosis and killing of *Cryptococcus neoformans* biofilm-derived cells by J774.16 macrophages is associated with fungal capsular production and surface modification. *Fungal Genet. Biol.* **2019**, *132*, 103258. [[CrossRef](#)]
20. Goldman, D.L.; Lee, S.C.; Casadevall, A. Tissue localization of *Cryptococcus neoformans* glucuronoxylomannan in the presence and absence of specific antibody. *Infect. Immun.* **1995**, *63*, 3448–3453. [[CrossRef](#)]
21. Bermas, A.; Geddes-McAlister, J. Combatting the evolution of antifungal resistance in *Cryptococcus neoformans*. *Mol. Microbiol.* **2020**, *114*, 721–734. [[CrossRef](#)]
22. Mourad, A.; Perfect, J.R. Present and Future Therapy of *Cryptococcus* infections. *J. Fungi* **2018**, *4*, 79. [[CrossRef](#)]
23. Srichatrapimuk, S.; Sungkanuparph, S. Integrated therapy for HIV and cryptococcosis. *AIDS Res. Ther.* **2016**, *13*, 42. [[CrossRef](#)]
24. Dong, K.; You, M.; Xu, J. Genetic Changes in Experimental Populations of a Hybrid in the *Cryptococcus neoformans* Species Complex. *Pathogens* **2020**, *9*, 3. [[CrossRef](#)]
25. Kauffman, C.A. Histoplasmosis. *Clin. Chest Med.* **2009**, *30*, 217–225. [[CrossRef](#)]
26. Queiroz-Telles, F.; Escuissato, D.L. Pulmonary paracoccidioidomycosis. *Semin. Respir. Crit. Care Med.* **2011**, *32*, 764–774. [[CrossRef](#)]
27. Wheat, L.J.; Azar, M.M.; Bahr, N.C.; Spec, A.; Relich, R.F.; Hage, C. Histoplasmosis. *Infect. Dis. Clin. N. Am.* **2016**, *30*, 207–227. [[CrossRef](#)]
28. Bagatin, M.C.; Rozada, A.M.F.; Rodrigues, F.A.V.; Bueno, P.S.A.; Santos, J.L.; Canduri, F.; Kioshima, É.S.; Seixas, F.A.V.; Basso, E.A.; Gauze, G.F. New 4-methoxy-naphthalene derivatives as promisor antifungal agents for paracoccidioidomycosis treatment. *Future Microbiol.* **2019**, *14*, 235–245. [[CrossRef](#)]
29. Martinez, R. New Trends in Paracoccidioidomycosis Epidemiology. *J. Fungi* **2017**, *3*, 1. [[CrossRef](#)]
30. do Carmo Silva, L.; de Oliveira, A.A.; de Souza, D.R.; Barbosa, K.L.; Freitas e Silva, K.S.; Carvalho Júnior, M.A.; Rocha, O.B.; Lima, R.M.; Santos, T.G.; Soares, C.M.; et al. Overview of Antifungal Drugs against Paracoccidioidomycosis: How Do We Start, Where Are We, and Where Are We Going? *J. Fungi* **2020**, *6*, 300. [[CrossRef](#)]
31. Shikanai-Yasuda, M.A.; Mendes, R.P.; Colombo, A.L.; Queiroz-Telles, F. Brazilian guidelines for the clinical management of paracoccidioidomycosis. *Rev. Soc. Bras. Med. Trop.* **2017**, *50*, 715–740. [[CrossRef](#)]
32. Azar, M.M.; Hage, C.A. Clinical Perspectives in the Diagnosis and Management of Histoplasmosis. *Clin. Chest Med.* **2017**, *38*, 403–415. [[CrossRef](#)] [[PubMed](#)]
33. Wheat, L.J.; Freifeld, A.G.; Kleiman, M.B.; Baddley, J.W.; McKinsey, D.S.; Loyd, J.E.; Kauffman, C.A. Clinical practice guidelines for the management of patients with histoplasmosis: 2007 update by the Infectious Diseases Society of America. *Clin. Infect. Dis.* **2007**, *45*, 807–825. [[CrossRef](#)] [[PubMed](#)]

34. Azar, M.M.; Loyd, J.L.; Relich, R.F.; Wheat, L.J.; Hage, C.A. Current Concepts in the Epidemiology, Diagnosis, and Management of Histoplasmosis Syndromes. *Semin. Respir. Crit. Care Med.* **2020**, *41*, 13–30. [[CrossRef](#)] [[PubMed](#)]
35. Costa-Orlandi, C.B.; Serafim-Pinto, A.; da Silva, P.B.; Bila, N.M.; Bonatti, J.L.d.C.; Scorzoni, L.; Singulani, J.d.L.; dos Santos, C.T.; Nazaré, A.C.; Chorilli, M.; et al. Incorporation of Nonyl 3,4-Dihydroxybenzoate Into Nanostructured Lipid Systems: Effective Alternative for Maintaining Anti-Dermatophytic and Antibiofilm Activities and Reducing Toxicity at High Concentrations. *Front. Microbiol.* **2020**, *11*, 1154. [[CrossRef](#)] [[PubMed](#)]
36. Gupta, A.K.; Stec, N.; Summerbell, R.C.; Shear, N.H.; Piguët, V.; Tosti, A.; Piraccini, B.M. Onychomycosis: A review. *J. Eur. Acad. Dermatol. Venereol.* **2020**, *34*, 1972–1990. [[CrossRef](#)]
37. Zhan, P.; Liu, W. The Changing Face of Dermatophytic Infections Worldwide. *Mycopathologia* **2017**, *182*, 77–86. [[CrossRef](#)]
38. Bila, N.M.; Costa-Orlandi, C.B.; Vaso, C.O.; Bonatti, J.L.C.; de Assis, L.R.; Regasini, L.O.; Fontana, C.R.; Fusco-Almeida, A.M.; Mendes-Giannini, M.J.S. 2-Hydroxychalcone as a Potent Compound and Photosensitizer Against Dermatophyte Biofilms. *Front. Cell. Infect. Microbiol.* **2021**, *11*, 679470. [[CrossRef](#)]
39. Gupta, A.K.; Cooper, E.A. Update in Antifungal Therapy of Dermatophytosis. *Mycopathologia* **2008**, *166*, 353–367. [[CrossRef](#)]
40. Costa-Orlandi, C.B.; Martinez, L.R.; Bila, N.M.; Friedman, J.M.; Friedman, A.J.; Mendes-Giannini, M.J.S.; Nosanchuk, J.D. Nitric Oxide-Releasing Nanoparticles Are Similar to Efinaconazole in Their Capacity to Eradicate *Trichophyton rubrum* Biofilms. *Front. Cell. Infect. Microbiol.* **2021**, *11*, 684150. [[CrossRef](#)]
41. Zhao, H.; Guo, W.; Quan, W.; Jiang, J.; Qu, B. Occurrence and levels of nitrofurans metabolites in sea cucumber from Dalian, China. *Food Addit. Contam. Part A* **2016**, *33*, 1672–1677. [[CrossRef](#)]
42. Krasavin, M.; Parchinsky, V.; Kantin, G.; Manicheva, O.; Dogonadze, M.; Vinogradova, T.; Karge, B.; Brønstrup, M. New nitrofurans amenable by isocyanide multicomponent chemistry are active against multidrug-resistant and poly-resistant *Mycobacterium tuberculosis*. *Bioorg. Med. Chem.* **2017**, *25*, 1867–1874. [[CrossRef](#)] [[PubMed](#)]
43. Claussen, K.; Stocks, E.; Bhat, D.; Fish, J.; Rubin, C.D. How Common Are Pulmonary and Hepatic Adverse Effects in Older Adults Prescribed Nitrofurantoin? *J. Am. Geriatr. Soc.* **2017**, *65*, 1316–1320. [[CrossRef](#)] [[PubMed](#)]
44. Aldeek, F.; Hsieh, K.C.; Ugochukwu, O.N.; Gerard, G.; Hammack, W. Accurate Quantitation and Analysis of Nitrofurans Metabolites, Chloramphenicol, and Florfenicol in Seafood by Ultrahigh-Performance Liquid Chromatography-Tandem Mass Spectrometry: Method Validation and Regulatory Samples. *J. Agric. Food Chem.* **2018**, *66*, 5018–5030. [[CrossRef](#)] [[PubMed](#)]
45. De Vita, D.; Friggeri, L.; D'Auria, F.D.; Pandolfi, F.; Piccoli, F.; Panella, S.; Palamara, A.T.; Simonetti, G.; Scipione, L.; Di Santo, R.; et al. Activity of caffeic acid derivatives against *Candida albicans* biofilm. *Bioorg. Med. Chem. Lett.* **2014**, *24*, 1502–1505. [[CrossRef](#)]
46. Kamal, A.; Hussaini, S.M.; Sucharitha, M.L.; Poornachandra, Y.; Sultana, F.; Ganesh Kumar, C. Synthesis and antimicrobial potential of nitrofurans-triazole congeners. *Org. Biomol. Chem.* **2015**, *13*, 9388–9397. [[CrossRef](#)]
47. De Vita, D.; Simonetti, G.; Pandolfi, F.; Costi, R.; Di Santo, R.; D'Auria, F.D.; Scipione, L. Exploring the anti-biofilm activity of cinnamic acid derivatives in *Candida albicans*. *Bioorg. Med. Chem. Lett.* **2016**, *26*, 5931–5935. [[CrossRef](#)]
48. Tangallapally, R.P.; Yendapally, R.; Lee, R.E.; Hevener, K.; Jones, V.C.; Lenaerts, A.J.; McNeil, M.R.; Wang, Y.; Franzblau, S. Synthesis and evaluation of nitrofuranyl amides as novel antituberculosis agents. *J. Med. Chem.* **2004**, *47*, 5276–5283. [[CrossRef](#)]
49. Gallardo-Macias, R.; Kumar, P.; Jaskowski, M.; Richmann, T.; Shrestha, R.; Russo, R.; Singleton, E.; Zimmerman, M.D.; Ho, H.P.; Dartois, V.; et al. Optimization of N-benzyl-5-nitrofurans-2-carboxamide as an antitubercular agent. *Bioorg. Med. Chem. Lett.* **2019**, *29*, 601–606. [[CrossRef](#)]
50. Arias, D.G.; Herrera, F.E.; Garay, A.S.; Rodrigues, D.; Forastieri, P.S.; Luna, L.E.; Bürgi, M.D.; Prieto, C.; Iglesias, A.A.; Cravero, R.M.; et al. Rational design of nitrofurans derivatives: Synthesis and valuation as inhibitors of *Trypanosoma cruzi* trypanothione reductase. *Eur. J. Med. Chem.* **2017**, *125*, 1088–1097. [[CrossRef](#)]
51. Pandolfi, F.; D'Acerno, F.; Bortolami, M.; De Vita, D.; Gallo, F.; De Meo, A.; Di Santo, R.; Costi, R.; Simonetti, G.; Scipione, L. Searching for new agents active against *Candida albicans* biofilm: A series of indole derivatives, design, synthesis and biological evaluation. *Eur. J. Med. Chem.* **2019**, *165*, 93–106. [[CrossRef](#)]
52. Jin, H.; Geng, Y.; Yu, Z.; Tao, K.; Hou, T. Lead optimization and anti-plant pathogenic fungi activities of daphneolone analogues from *Stellera chamaejasme* L. *Pestic. Biochem. Physiol.* **2009**, *93*, 133–137. [[CrossRef](#)]
53. Gomes, M.N.; Braga, R.C.; Grzelak, E.M.; Neves, B.J.; Muratov, E.; Ma, R.; Klein, L.L.; Cho, S.; Oliveira, G.R.; Franzblau, S.G.; et al. QSAR-driven design, synthesis and discovery of potent chalcone derivatives with antitubercular activity. *Eur. J. Med. Chem.* **2017**, *137*, 126–138. [[CrossRef](#)] [[PubMed](#)]
54. Press, J.B.; Wright, W.B., Jr.; Chan, P.S.; Haug, M.F.; Marsico, J.W.; Tomcufcik, A.S. Thromboxane synthetase inhibitors and antihypertensive agents. 3. N-[(1H-imidazol-1-yl)alkyl]heteroaryl amides as potent enzyme inhibitors. *J. Med. Chem.* **1987**, *30*, 1036–1040. [[CrossRef](#)]
55. Tawari, N.R.; Bairwa, R.; Ray, M.K.; Rajan, M.G.R.; Degani, M.S. Design, synthesis, and biological evaluation of 4-(5-nitrofurans-2-yl)prop-2-en-1-one derivatives as potent antitubercular agents. *Bioorg. Med. Chem. Lett.* **2010**, *20*, 6175–6178. [[CrossRef](#)]
56. Holla, B.S.; Veerendra, B.; Shivananda, M.K. Non-linear optical properties of new arylfuranylpropenones. *J. Cryst. Growth* **2004**, *263*, 532–535. [[CrossRef](#)]
57. de Macedo, P.M.; Teixeira, M.M.; Barker, B.M.; Zancopé-Oliveira, R.M.; Almeida-Paes, R.; do Valle, A.C.F. Clinical features and genetic background of the sympatric species *Paracoccidioides brasiliensis* and *Paracoccidioides americana*. *PLoS Negl. Trop. Dis.* **2019**, *13*, e0007309. [[CrossRef](#)]

58. Clinical and Laboratory Standards Institute. *Reference Method for Broth Dilution Antifungal Susceptibility Testing of Yeasts (M27-A3)*; Clinical and Laboratory Standards Institute: Wayne, PA, USA, 2008.
59. Baltazar, L.M.; Zamith-Miranda, D.; Burnet, M.C.; Choi, H.; Nimrichter, L.; Nakayasu, E.S.; Nosanchuk, J.D. Concentration-dependent protein loading of extracellular vesicles released by *Histoplasma capsulatum* after antibody treatment and its modulatory action upon macrophages. *Sci. Rep.* **2018**, *8*, 8065. [[CrossRef](#)]
60. Gonçalves, L.N.C.; Costa-Orlandi, C.B.; Bila, N.M.; Vaso, C.O.; Da Silva, R.A.M.; Mendes-Giannini, M.J.S.; Taylor, M.L.; Fusco-Almeida, A.M. Biofilm Formation by *Histoplasma capsulatum* in Different Culture Media and Oxygen Atmospheres. *Front. Microbiol.* **2020**, *11*, 1455. [[CrossRef](#)]
61. de Paula e Silva, A.C.A.; Oliveira, H.C.; Silva, J.F.; Sangalli-Leite, F.; Scorzoni, L.; Fusco-Almeida, A.M.; Mendes-Giannini, M.J.S. Microplate alamarBlue Assay for Paracoccidioides Susceptibility Testing. *J. Clin. Microbiol.* **2013**, *51*, 1250–1252. [[CrossRef](#)]
62. Costa-Orlandi, C.B.; Sardi, J.C.O.; Santos, C.T.; Fusco-Almeida, A.M.; Mendes-Giannini, M.J.S. *In vitro* characterization of *Trichophyton rubrum* and *T. mentagrophytes* biofilms. *Biofouling* **2014**, *30*, 719–727. [[CrossRef](#)]
63. Li, R.K.; Ciblak, M.A.; Nordoff, N.; Pasarell, L.; Warnock, D.W.; McGinnis, M.R. *In vitro* activities of voriconazole, itraconazole, and amphotericin B against *Blastomyces dermatitidis*, *Coccidioides immitis*, and *Histoplasma capsulatum*. *Antimicrob. Agents Chemother.* **2000**, *44*, 1734–1736. [[CrossRef](#)] [[PubMed](#)]
64. Wheat, L.J.; Connolly, P.; Smedema, M.; Brizendine, E.; Hafner, R.; AIDS Clinical Trials Group and the Mycoses Study Group of the National Institute of Allergy and Infectious Diseases. Emergence of Resistance to Fluconazole as a Cause of Failure during Treatment of Histoplasmosis in Patients with Acquired Immunodeficiency Disease Syndrome. *Clin. Infect. Dis.* **2001**, *33*, 1910–1913. [[CrossRef](#)] [[PubMed](#)]
65. Kathuria, S.; Singh, P.K.; Meis, J.F.; Chowdhary, A. *In vitro* antifungal susceptibility profile and correlation of mycelial and yeast forms of molecularly characterized *Histoplasma capsulatum* strains from India. *Antimicrob. Agents Chemother.* **2014**, *58*, 5613–5616. [[CrossRef](#)] [[PubMed](#)]
66. Nakano, N.; Fukuhara-Takaki, K.; Jono, T.; Nakajou, K.; Eto, N.; Horiuchi, S.; Takeya, M.; Nagai, R. Association of advanced glycation end products with A549 cells, a human pulmonary epithelial cell line, is mediated by a receptor distinct from the scavenger receptor family and RAGE. *J. Biochem.* **2006**, *139*, 821–829. [[CrossRef](#)]
67. Xiao, J.; Zhang, Y.; Wang, J.; Yu, W.; Wang, W.; Ma, X. Monitoring of Cell Viability and Proliferation in Hydrogel-Encapsulated System by Resazurin Assay. *Appl. Biochem. Biotechnol.* **2010**, *162*, 1996–2007. [[CrossRef](#)]
68. Scorzoni, L.; Sangalli-Leite, F.; de Lacorte Singulani, J.; de Paula e Silva, A.C.A.; Costa-Orlandi, C.B.; Fusco-Almeida, A.M.; Mendes-Giannini, M.J.S. Searching new antifungals: The use of *in vitro* and *in vivo* methods for evaluation of natural compounds. *J. Microbiol. Methods* **2016**, *123*, 68–78. [[CrossRef](#)]
69. Abdullah, N.A.; Ja'afar, F.; Yasin, H.M.; Taha, H.; Petalcorin, M.I.R.; Mamit, M.H.; Kusri, E.; Usman, A. Physicochemical analyses, antioxidant, antibacterial, and toxicity of propolis particles produced by stingless bee *Heterotrigona itama* found in Brunei Darussalam. *Heliyon* **2019**, *5*, e02476. [[CrossRef](#)]
70. Medina-Alarcón, K.P.; Singulani, J.L.; Voltan, A.R.; Sardi, J.C.O.; Petrónio, M.S.; Santos, M.B.; Polaquini, C.R.; Regasini, L.O.; Bolzani, V.S.; da Silva, D.H.S.; et al. Alkyl Protocatechuate-Loaded Nanostructured Lipid Systems as a Treatment Strategy for *Paracoccidioides brasiliensis* and *Paracoccidioides lutzii* *In Vitro*. *Front. Microbiol.* **2017**, *8*, 1048. [[CrossRef](#)]
71. Scorzoni, L.; de Lucas, M.P.; Mesa-Arango, A.C.; Fusco-Almeida, A.M.; Lozano, E.; Cuenca-Estrella, M.; Mendes-Giannini, M.J.; Zaragoza, O. Antifungal efficacy during *Candida krusei* infection in non-conventional models correlates with the yeast *in vitro* susceptibility profile. *PLoS ONE* **2013**, *8*, e60047. [[CrossRef](#)]
72. Sun, S.; Hoy, M.J.; Heitman, J. Fungal pathogens. *Curr. Biol.* **2020**, *30*, R1163–R1169. [[CrossRef](#)]
73. Gupta, A.K.; Stec, N. Recent advances in therapies for onychomycosis and its management. *F1000Research* **2019**, *8*, 968. [[CrossRef](#)] [[PubMed](#)]
74. Grässer, U.; Bubel, M.; Sossong, D.; Oberringer, M.; Pohlemann, T.; Metzger, W. Dissociation of mono- and co-culture spheroids into single cells for subsequent flow cytometric analysis. *Ann. Anat.* **2018**, *216*, 1–8. [[CrossRef](#)] [[PubMed](#)]
75. Molinaro, E.M.; Caputo, L.F.G.; Amendoeira, M.R.R. *Conceitos e Métodos Para Formação de Profissionais em Laboratório de Saúde*; Escola Politécnica de Saúde Joaquim Venâncio, I.O.C.: Rio de Janeiro, Brazil, 2012.
76. Hunt, P.R. The *C. elegans* model in toxicity testing. *J. Appl. Toxicol.* **2017**, *37*, 50–59. [[CrossRef](#)] [[PubMed](#)]
77. Singulani, J.L.; Scorzoni, L.; Gomes, P.C.; Nazaré, A.C.; Polaquini, C.R.; Regasini, L.O.; Fusco-Almeida, A.M.; Mendes-Giannini, M.J.S. Activity of gallic acid and its ester derivatives in *Caenorhabditis elegans* and zebrafish (*Danio rerio*) models. *Future Med. Chem.* **2017**, *9*, 1863–1872. [[CrossRef](#)]
78. Bagla, V.P.; McGaw, L.J.; Elgorashi, E.E.; Eloff, J.N. Antimicrobial activity, toxicity and selectivity index of two biflavonoids and a flavone isolated from *Podocarpus henkelii* (Podocarpaceae) leaves. *BMC Complementary Altern. Med.* **2014**, *14*, 383. [[CrossRef](#)]
79. Ochoa-Pacheco, A.; Escalona Arranz, J.C.; Beaven, M.; Peres-Roses, R.; Gámez, Y.M.; Camacho-Pozo, M.I.; Mauray, G.L.; de Macedo, M.B.; Cos, P.; Tavares, J.F.; et al. Bioassay-guided *In vitro* Study of the Antimicrobial and Cytotoxic Properties of the Leaves from *Excoecaria Lucida* Sw. *Pharmacogn. Res.* **2017**, *9*, 396–400. [[CrossRef](#)]
80. Nielsen, K.; Vedula, P.; Smith, K.D.; Meya, D.B.; Garvey, E.P.; Hoekstra, W.J.; Schotzinger, R.J.; Boulware, D.R. Activity of VT-1129 against *Cryptococcus neoformans* clinical isolates with high fluconazole MICs. *Med. Mycol.* **2016**, *55*, 453–456. [[CrossRef](#)]
81. May, R.C.; Stone, N.R.H.; Wiesner, D.L.; Bicanic, T.; Nielsen, K. *Cryptococcus*: From environmental saprophyte to global pathogen. *Nat. Rev. Microbiol.* **2016**, *14*, 106–117. [[CrossRef](#)]

82. Smith, K.D.; Achan, B.; Hullsiek, K.H.; McDonald, T.R.; Okagaki, L.H.; Alhadab, A.A.; Akampurira, A.; Rhein, J.R.; Meya, D.B.; Boulware, D.R.; et al. Increased Antifungal Drug Resistance in Clinical Isolates of *Cryptococcus neoformans* in Uganda. *Antimicrob. Agents Chemother.* **2015**, *59*, 7197–7204. [[CrossRef](#)]
83. Chen, Y.-C.; Chang, T.-Y.; Liu, J.-W.; Chen, F.-J.; Chien, C.-C.; Lee, C.-H.; Lu, C.-H. Increasing trend of fluconazole-non-susceptible *Cryptococcus neoformans* in patients with invasive cryptococcosis: A 12-year longitudinal study. *BMC Infect. Dis.* **2015**, *15*, 277. [[CrossRef](#)]
84. Pontón, J.; Rüchel, R.; Clemons, K.V.; Coleman, D.C.; Grillot, R.; Guarro, J.; Aldebert, D.; Ambroise-Thomas, P.; Cano, J.; Carrillo-Muñoz, A.J.; et al. Emerging pathogens. *Med. Mycol.* **2000**, *38*, 225–236. [[CrossRef](#)]
85. Wheat, L.J.; Connolly, P.; Smedema, M.; Durkin, M.; Brizendine, E.; Mann, P.; Patel, R.; McNicholas, P.M.; Goldman, M. Activity of newer triazoles against *Histoplasma capsulatum* from patients with AIDS who failed fluconazole. *J. Antimicrob. Chemother.* **2006**, *57*, 1235–1239. [[CrossRef](#)]